

# Effects of Flame Curvature on Chemical Reactions in Rich Hydrogen-Air Premixed Flame

Yasuhiro Mizobuchi<sup>\*</sup>, Tadao Takeno, Shingo Matsuyama, Junji Shinjo, Satoru Ogawa

Aerospace Research and Development Directorate, Japan Aerospace Exploration Agency,  
7-44-1, Jindaiji-higashi, Chofu, Tokyo, Japan

## 1 Introduction

Unusual molecular diffusion produces some unique behavior of off-stoichiometric premixed flames, and has been discussed as a cause of the cellular or polyhedral flames [1]. However, the detailed processes leading to these phenomena, called selective diffusion or preferential diffusion, have not been fully understood yet. The most popular explanation, so called Lewis number effect, is based on the accelerated mass diffusion of the deficient species. However, the explanation is based on the rather simplified system, with global one-step reaction, and small number of participating species such as fuel, oxidizer and product. In the actual flames, on the other hand, the chemical reaction proceeds through the complicated multi-step reactions, and there exist so many species including radicals, intermediate products, and so on. How the flame curvature should affect the chemical reaction proceeding in the flame. This is the problem to be studied.

One possible difficulty in the experimental study is that it is very hard to reveal roles played by respective chemical species in the chemical reaction involved in the flame. On the other hand, the recent progress in numerical calculation is remarkable, and now it becomes possible to reproduce what actually happens in the flame by the large calculation with the detailed chemical kinetics and accurate transport properties [2-4]. In this kind of calculation it is rather easy to identify the roles played by the respective species in the observed flame behavior by means of the detailed data analysis.

When we want to understand the above mentioned unique flame behavior, it should be natural to adopt some steady flames. However, any steady 2-D or 3-D laminar flames should be accompanied by some kind of flow deformation so as to stabilize the flame and are inevitably subjected to the consequent flame stretch. It is preferable to adopt the flame strictly one-dimensional and free from the stretch, at least in the beginning. One example is the 1-D freely propagating flame in the slowly moving mixture. This is the very flame adopted in our study. The strictly 1-D flame is freely propagating against a slowly moving rich hydrogen air mixture. A high speed small jet of the same mixture is injected toward the flame and the subsequent time dependent flame behavior has been analyzed in terms of the 2-D numerical calculation.

## 2 Numerical model

A rich hydrogen-air mixture of equivalence ratio 4.5 is flowing upward with the uniform velocity of 1.38 m/sec. The temperature and the pressure are 300K and 1atm, respectively. The mixture is ignited at the downstream end, and the uniform 1-D flame is established and begins to propagate upward. However, the burning velocity of the mixture is very near to 1.38 m/sec and therefore the 1-D flame remains almost steadily at the original position. Then a small volume of the same mixture is injected with velocity of 20.0 m/sec towards the 1-D flame, through an injector of 1.5 mm width, placed at the upstream end. The jet encounters with the flame to produce deformation of the flame configuration. The configuration at the subsequent six stages, are illustrated in Fig. 1, with the contours of H<sub>2</sub> consumption rate represented by color. As a result of the encounter, the flame begins to deform to develop some unique flame shape like a water drop, which is cut off at the base subsequently to produce an isolated flame island. In the course of time, the flame island disappears, and finally the deformed 1-D flame comes back again to the original straight 1-D flame. At each instants of this event, the flame responds to the jet instantaneously to develop the flame configuration of that instant. The characteristic times of the involved chemical reactions and the transport phenomena are so small as compared to the characteristic time of the deformation, the quasi-steady state is almost established in the flame structure of the instant. It should be noticed that when the flame develops the bulge shape (stage e), the local fuel consumption rate at the top increases over that of the normal 1-D flame. Now we will study the cause of this increase.

In this study, the chemical reaction mechanism of 9-species (H<sub>2</sub>, O<sub>2</sub>, OH, H<sub>2</sub>O, H, O, H<sub>2</sub>O<sub>2</sub>, HO<sub>2</sub>, N<sub>2</sub>) and 21-reaction model [5] shown in Table 1 is used. The transport properties as well as the thermodynamic properties, provided by CHEMKIN [6] are used as they are. The air is assumed to be composed of 21% O<sub>2</sub> and 79% N<sub>2</sub> in volume. The governing equations are the compressible Navier-Stokes equations coupled with the conservation equations of the 9 chemical species. They are discretized in a finite-volume formulation. The convective terms are evaluated using an upwind numerical flux based on Roe's approximate Riemann solver [7, 8]. The inflow and outflow boundary conditions are given based on the NSCBC method [9]. At the inflow boundary, the velocity, the temperature and the gas composition are imposed, and the non-reflecting condition with modification for the constant pressure at infinity is imposed at the outflow boundary. The right and left boundaries are symmetric boundaries. The computational grid is rectangular and the grid spacing is 25  $\mu$  m.

## 3 Numerical results

### 3.1 Time dependent Flame Behavior

Figure 1 shows the flame configuration at the subsequent six stages with the contours of H<sub>2</sub> consumption rate represented by color. As a result of the encounter, the flame begins to deform to develop some unique flame shape like a water drop, which is cut off at the base subsequently to produce an isolated flame island. In the course of time, the flame island disappears, and the deformed 1-D flame finally comes back again to the original straight 1-D flame. It should be noticed that when the flame develops the bulge shape, the local fuel consumption rate at the top increases over that of the normal 1-D flame. Now the flame configuration at a certain stage is analyzed in the following.

### 3.2 Increase in H<sub>2</sub> consumption rate

Figure 2 shows the local H<sub>2</sub> consumption rate as a function of the temperature at the same position. The data points are taken from the whole flame structure at the instant e) in Fig. 1, when the flame takes the configuration of water drop shown in a small inset. The solid curve represents the relation of 1-D normal flame calculated using [9], with the open circle on the abscissa indicates the adiabatic flame temperature  $T^{\text{ad}}$ . The consumption rates are made non-dimensional by the maximum value of the 1-D flame. In the figure,  $\kappa$  represents the curvature defined by the 2-D temperature distribution,

$$\kappa = \nabla \cdot \mathbf{n}, \quad \mathbf{n} = \text{grad } T / |\text{grad } T|$$

where  $\mathbf{n}$  is the unit vector normal to the temperature contours. The positive curvature means that the flame is concave towards the unburned mixture. Most of the red points, deviated from the solid curve, come from the bulge portion of the water drop shape, where the local flame is curved and is subject to

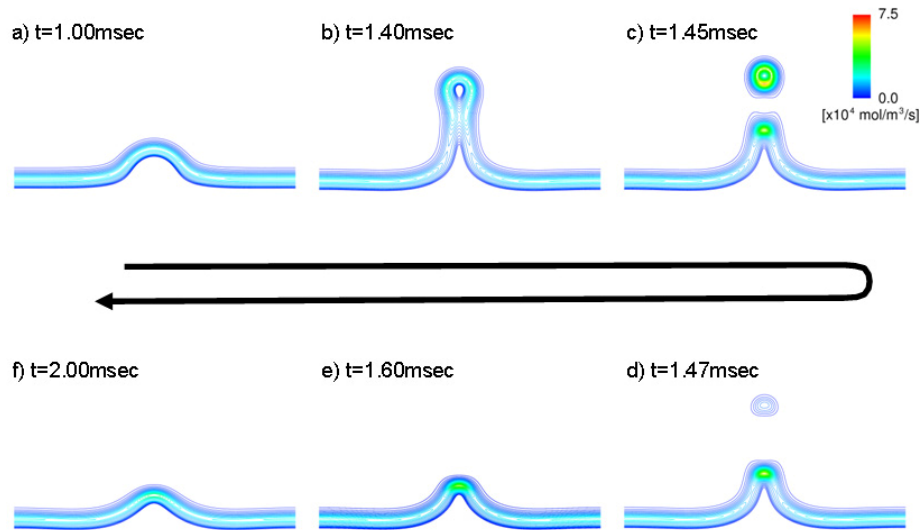


Figure 1. Time-sequenced flame behavior. The flame configurations at six instants are represented by contours of  $\text{H}_2$  consumption rate.

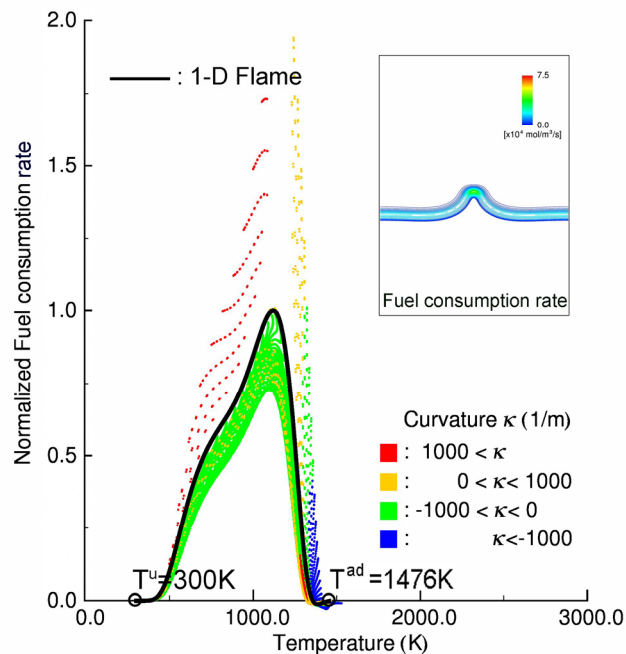


Figure 2. Local  $\text{H}_2$  consumption rate as a function of the temperature at that position. The data points are taken from the whole flame at the instant e), when the flame takes the configuration of water drop shape shown in a small inset. The solid curve represents the relation of the 1-D normal flame, with the open circle on the abscissa indicates the adiabatic flame temperature  $T^{\text{ad}}$ .

the curvature. As is seen in the figure, the local consumption rate exceeds considerably over that of the 1-D flame, with the rather large positive curvature ( $\kappa > 1,000$ ) in the relatively low temperature region below 1,100 K. The increase is very large and the maximum value is almost twice that of the 1-D flame. On the other hand, it also increases for the small positive curvature ( $0 < \kappa < 1,000$ ) in the relatively high temperature region. In the both regions, the negative curvature decreases the consumption rate. These features suggest that the curvature effect is very complicated. In any way, the 2-D flame configuration clearly affects the chemical reactions proceeding inside the flame structure. The low temperature increase has also been observed in the previous study [10] and analyzed to reveal that, after all, the accelerated mass diffusion of H species to the reaction zone is responsible for this increase.

Figure 3 presents the oxygen concentration distribution at the same instant. The left 2-D figure reveals that the local oxygen concentration of the bulge portion remains almost the same with that of the 1-D straight portion. The right figure presents the detailed comparison of the local oxygen concentration with that of the 1-D flame. The local concentration normalized by that of air is plotted as a function of the temperature at the same position. The solid curve represents that of 1-D normal flame, with the open circle on the abscissa indicates the adiabatic flame temperature  $T^{\text{ad}}$ . We notice that when the flame develops concave curvature larger than 1,000, the local oxygen concentration exceeds over that of the 1-D flame. However, the excess is not large enough to explain the large increase of the local fuel consumption rate shown before. Now we understand that the local increase of  $\text{H}_2$  consumption rate is not provided by the increased temperature nor the increased oxygen concentration.

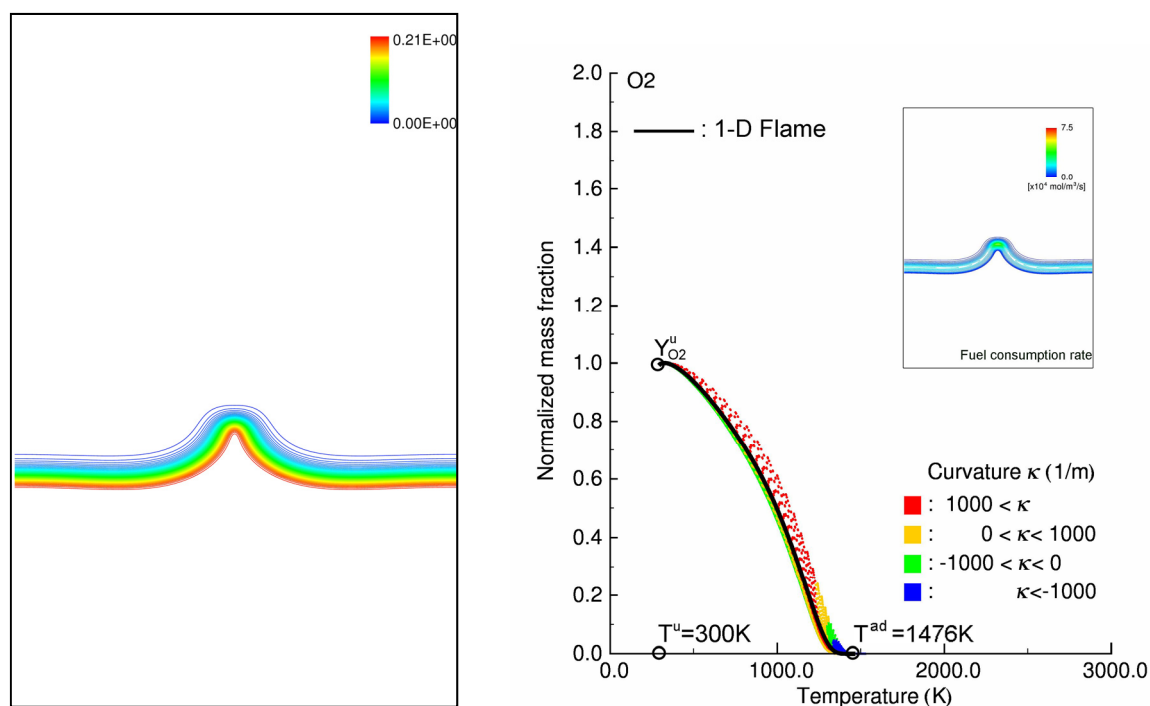


Figure 3. The flame structure at the instant of e). The left figure presents 2-D  $\text{O}_2$  concentration contours, and the right local  $\text{O}_2$  mass fraction as a function of temperature.

### 3.3 Increase in OH concentration

Figure 4 shows OH mass fraction as a function of the temperature at the same position. The data points represent the data at the same instant with Figs. 1-3. The solid curve and the open circles represent those of the 1-D flame, here again, and  $Y_{\text{OH}}^{\text{ad}}$  is the equilibrium value at  $T^{\text{ad}}$ . We see that the

flame curvature provides extraordinary increases in OH concentration at the lower and the higher temperature regions. In our previous study[10], we have made an analysis to understand the lower increase and have found that the increase of OH mass fraction is provided by the increase in R11 reaction rate.



However, this rapid production is followed by a rapid OH consumption by R3 and the net production rate remains almost zero in the whole reaction zone. We now understand that the rapid increase in H<sub>2</sub> consumption rate is provided by the increased OH concentration through R11. The next problem is the reason why these reaction rates are accelerated. We are still engaged in the analysis to answer the question.

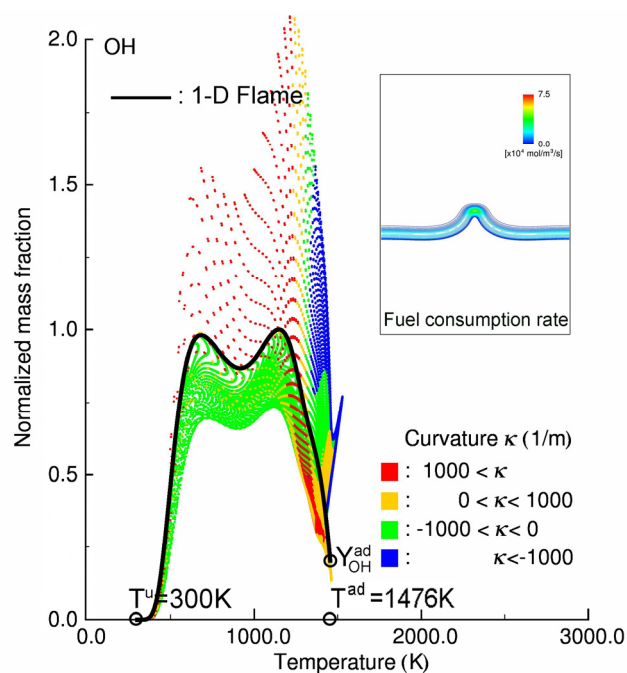


Figure 4. Local normalized OH mass fraction as a function of the temperature at that position. The data points are taken from the whole flame. The open circle  $Y_{\text{OH}}^{\text{ad}}$  indicates downstream equilibrium value of 1-D flame.

#### 4 Some Concluding Remarks

The effect of flame configuration on the fuel consumption rate has been studied by means of 2-D numerical calculation with detailed chemical kinetics and accurate transport properties for a rich hydrogen-air mixture. It has been found that the local fuel consumption rate increases or decreases at the portion where the flame develops curvature. These increase or decrease cannot be explained in terms of the simplified theory based on the Lewis number effect. Instead, the flame configuration actually affects the chemical reactions proceeding inside the flame structure, and further study is being conducted to understand the effect.

#### References

- [1] Gaydon, A.G. and Wolfhard, H.G., "FLAMES, Their structure, radiation and temperature," Third Edition Revised, Chapman and Hall Ltd. London, p. 32(1970).

- [2] Mizobuchi, Y., Tachibana, S., Shinjo, J., Ogawa, S. and Takeno, T., "A Numerical Analysis on Structure of Turbulent Hydrogen Jet Lifted Flame," *Proc. Combust. Inst.* 29: 2009-2015 (2002).
- [3] Bell, J.B., Day, M. S., Shepherd, I.G., Johnson, M.R., Cheng R.K., Grcar, J.F., Beckner, V.E. and Lijewski, M.J., "Numerical simulation of a laboratory-scale turbulent V flame," *Proc. Nat. Acad. Sci. USA*, 102(29):10006-10011 (2005).
- [4] Westbrook, C.K. et al., "Computational combustion," *Proc. Combust. Inst.* 32: 2009-2015 (2008).
- [5] Williams, F.A. "Chemical-Kinetic Simplifications for Lean Hydrogen Deflagrations," 4<sup>TH</sup> ISFEH (Corsica, 2009).
- [6] Kee, R. J., Grcar, J. F., Smooke, M. D. and Miller, J. A., "FORTRAN program for modeling steady one dimensional flames," Sandia Report SAND85-8240 (1985).
- [7] Roe, P.L., "Approximate Riemann Solvers, Parameter Vectors, and Difference Scheme," *J. Comp. Phys.*, 43:357-372 (1981).
- [8] Wada, Y., Ogawa, S. and Ishiguro, T., "A Generalized Roe's Approximate Riemann Solver for Chemically Reacting Flows," *AIAA paper 89-0202* (1989).
- [9] Poinso, T. J., and Lele, S.K., "Boundary Conditions for Direct Simulations of Compressible Viscous Flows," *J. Comp. Phys.* 101:104-129(1992).
- [10] Mizobuchi, Y., Takeno, T., Matsuyama, S., Shinjo, J. and Ogawa, S., "Effects of Flame Curvature on chemical Reactions in Rich Hydrogen-Air Premixed Flame," *Proc. of Sixth International Symposium on Scale Modeling* (Hawaii, 2009).

Table 1: Chemical reaction mechanism adopted in this calculation [5].

	Reaction
R1	$H + O_2 = OH + O$
R2	$H_2 + O = OH + H$
R3	$H_2 + OH = H_2O + H$
R4	$H_2O + O = OH + OH$
R5	$H + H + M = H_2 + M$
R6	$H + OH + M = H_2O + M$
R7	$O + O + M = O_2 + M$
R8	$H + O + M = OH + M$
R9	$O + OH + M = HO_2 + M$
R10	$H + O_2 + M = HO_2 + M$
R11	$HO_2 + H = OH + OH$
R12	$HO_2 + H = H_2 + O_2$
R13	$HO_2 + H = H_2O + O$
R14	$HO_2 + O = OH + O_2$
R15	$HO_2 + OH = H_2O + O_2$
R16	$OH + OH + M = H_2O_2 + M$
R17	$HO_2 + HO_2 = H_2O_2 + O_2$
R18	$H_2O_2 + H = HO_2 + H_2$
R19	$H_2O_2 + H = H_2O + OH$
R20	$H_2O_2 + OH = H_2O + HO_2$
R21	$H_2O_2 + O = HO_2 + OH$